The H(b1)···H(b2) nonbonding distance (2.339 (3) Å) is comparable to those found in other $M(\mu\text{-}H)_2M$ fragments: 2.405 (3) Å in $[H_2W_2(CO)_8]^{2-}$,[10] 2.465 (14) Å in $H_2Rh_2[P(O\text{-}i\text{-}Pr)_3]_4$,[11] and 2.376 (3) Å in $H_2Os_3(CO)_{10}$.[12] These values, which were all obtained from accurate neutron diffraction analyses, seem to indicate that H···H distances in doubly bridged M–M bonds stay fairly constant at about 2.4 Å.

Finally, it should be mentioned that the present structure determination represents the most accurate measurement of a terminal Pt–H bond distance carried out to date (1.610 (2) Å). Earlier measurements (by X-ray diffraction) yielded values of 1.527,[2b] 1.66,[13] 1.78,[14] and 1.98 Å.[15]

Acknowledgment. This research was supported by the Petroleum Research Fund, administered by the American Chemical Society, and by the Consiglio Nazionale delle Ricerche (CNR), Rome. Work at Brookhaven National Laboratory was performed under contract with the U.S. Department of Energy. We wish to thank Dr. Thomas J. Emge, Joseph Henriques, Dr. Richard M. Kirchner, and Saeed I. Khan for assistance in parts of this work.

Registry No. $[H_3Pt_2(Ph_2PCH_2CH_2PPh_2)_2]^+[BPh_4]^-$, 88130-93-2.

Supplementary Material Available: Listings of the final atomic coordinates and anisotropic temperature factors (Table A), interatomic distances (Table B), bond angles (Table C), and average molecular parameters (Table D) for the neutron analysis (16 pages). Ordering information is given on any masthead page.

Department of Chemistry
University of Southern California
Los Angeles, California 90089
Michael Y. Chiang
Robert Bau*

Istituto di Chimica Analitica
Università di Sassari
Sassari 07100, Italy
Giovanni Minghetti*

Centro CNR
Dipartimento di Chimica Inorganica e Metallorganica
Università di Milano
Milano 20133, Italy
Anna Laura Bandini
Guido Banditelli

Chemistry Department
Brookhaven National Laboratory
Upton, New York 11973
Thomas F. Koetzle*

Received October 14, 1983

(10) Wei, C. Y.; Marks, M. W.; Bau, R.; Kirtley, S. W.; Bisson, D. E.; Henderson, M. E.; Koetzle, T. F. *Inorg. Chem.* **1982**, *21*, 2556.
(11) Teller, R. G.; Williams, J. M.; Koetzle, T. F.; Burch, R. R.; Gavin, R. M.; Muetterties, E. L. *Inorg. Chem.* **1981**, *20*, 1806.
(12) Broach, R. W.; Williams, J. M. *Inorg. Chem.* **1979**, *18*, 314.
(13) Kane, A. R.; Guggenberger, L. J.; Muetterties, E. L. *J. Am. Chem. Soc.* **1970**, *92*, 2571.
(14) Auburn, M.; Ciriano, M.; Howard, J. A. K.; Murray, M.; Pugh, N. J.; Spencer, J. L.; Stone, F. G. A.; Woodward, P. *J. Chem. Soc., Dalton Trans.* **1980**, 659.
(15) Furlani, A.; Licoccia, S.; Russo, M. V.; Villa, A. C.; Guastini, C. *J. Chem. Soc., Dalton Trans.* **1982**, 2449.
(16) Molecular plots were generated by the program ORTEP-II: Johnson, C. K. *Oak Ridge Natl. Lab. [Rep.], ORNL (U.S.)* **1976**, *ORNL-5138*.

Articles

Contribution from the Department of Chemistry,
Texas A&M University, College Station, Texas 77843

Characterization of a Fischer–Tropsch Catalyst Prepared by Decarbonylation of Dodecacarbonyltetracobalt on Alumina

GREGORY F. MEYERS and MICHAEL B. HALL*

Received September 30, 1982

When supported on partially dehydroxylated $\gamma\text{-}Al_2O_3$, $Co_4(CO)_{12}$ is an active Fischer–Tropsch (F-T) catalyst. The catalyst is deposited out of hexane solution, thermally decarbonylated, and reacted in the presence of 3:2 H_2–CO at 250 °C. The zerovalent cluster, when initially deposited on the support, is extremely sensitive to oxidation. X-ray photoelectron spectroscopy (XPS) indicates that the extent of oxidation is to Co(II). XPS of the decarbonylated and used catalyst indicates the presence of reduced cobalt species in addition to Co(II). This latter observation is supported by laser-induced mass spectroscopy (LIMS). After thermal decarbonylation, the LIMS shows that cobalt clusters, Co_x (x = 2, 5, 6, 7), are present. After one F-T cycle, only Co_4 clusters of the type $Co_4(CO)_x$ (x = 2–6) and cluster carbides, $Co_4(CO)_xC$ (x = 0, 1, 2, 4, 11), are present on the surface. Under mild conditions, the catalyst after one F-T cycle cannot be completely reduced to Co(0) nor oxidized to Co(III) as evidenced by the XPS of H_2- and O_2-treated samples. Transmission electron microscopy (TEM) showed no visible Co particles (>10 nm) on any sample.

Currently, there is a renewed interest in the Fischer–Tropsch (F-T) synthesis[1,2] as a potentially viable alternative to the production of gasoline and chemical feedstocks.[3] Typically, the group 8 metals show the greatest specific activity for the reaction;[4] however, these catalysts are derived from mononuclear salts in which the metal is initially in a relatively high oxidation state. Pretreatment of the supported metal traditionally involves high-temperature calcination and reduction, which can lead to metal sintering (and, therefore, poor dispersion).[5] Recently, it has been demonstrated that catalysts derived from mononuclear group 6[6] and polynuclear group 8[7]

(1) Storch, H. H.; Golumbic, N.; Anderson, R. B. "The Fischer-Tropsch and Related Synthesis"; Wiley: New York, 1951.
(2) Masters, C. *Adv. Organomet. Chem.* **1979**, *17*, 61.
(3) (a) Haggin, J. *Chem. Eng. News* **1981**, *59* (Oct 26), 22. (b) King, R. B.; Cusumano, J. A.; Garten, R. L., *Catal. Rev.—Sci. Eng.* **1981**, *23* (1/2), 233. (c) Pruett, R. L. *Science (Washington, D.C.)* **1981**, *211*, 11.
(4) (a) Vannice, M. A. *Adv. Chem. Ser.* **1977**, *No. 163*, 15. (b) Vannice, M. A. *J. Catal.* **1975**, *37*, 449.
(5) (a) Anderson, J. R. "Structure of Metallic Catalysts"; Academic Press: New York, 1975. (b) Geus, J. W. "Sintering and Catalysis"; Kucynski, G. C., Ed.; Plenum Press: New York, 1975.

0020-1669/84/1323-0124$01.50/0

metal carbonyls (in which the metal is initially zerovalent) may be deposited on high-surface-area refractory oxides with very high dispersions and with retention of the metal in a relatively low oxidation state.

The choice of metal cluster compounds, in particular, is attractive because of possible cooperative effects between metal centers[8,9] and because of the close analogy between discrete metal clusters and metal surfaces with chemisorbed molecules.[10] While a great deal of valuable information has been reported concerning the chemisorptive decomposition of metal carbonyls on high-surface-area metal oxide supports,[11] only a handful of investigators are beginning to examine metal carbonyl clusters as possible heterogeneous Fischer–Tropsch catalysts. In particular, supported $Fe_3(CO)_{12}$[12a-d] and $Ru_3(CO)_{12}$,[12a,b,d-f] $Os_3(CO)_{12}$,[12a,g] $Co_2(CO)_8$,[12d,h,i] $Rh_4(CO)_{12}$[12a,j-l] $Rh_6(CO)_{16}$,[12a,j-l] and $Ir_4(CO)_{12}$[12l] have been reported to convert CO/H_2 mixtures to F-T products. In addition, decomposition of many polynuclear metal carbonyls onto oxide supports in the presence of H_2[13a] or CO[13b] results in the formation of hydrocarbons.

Of all the neutral metal carbonyls, $Co_4(CO)_{12}$ has received little attention presumably due to its pyrophoric nature. However, $Co_4(CO)_{12}$ has been reported to catalyze the homogeneous dimerization of norbornadiene,[14a] the homogeneous hydroformylation and hydroesterification of 1-octene,[14b] and the heterogeneous hydroformylation of ethylene and propylene.[14c,d] In this paper we report on the heterogeneous Fischer–Tropsch synthesis using $Co_4(CO)_{12}$ supported on γ-Al_2O_3. The techniques employed are X-ray photoelectron spectroscopy (XPS), laser-induced mass spectroscopy (LIMS), and transmission electron microscopy (TEM).

Experimental Section

Materials. Dodecacarbonyltetracobalt, $Co_4(CO)_{12}$, was prepared from dicobaltoctacarbonyl, $Co_2(CO)_8$, by the method of Chini et al.,[15] and the product was sublimed (36 °C, 0.25 torr) prior to use. Its purity was checked by IR investigation of the carbonyl stretching region.[16] Hexane (mixture of isomers, Fischer reagent) was distilled from sodium–benzophenone and stored under dry nitrogen in a glovebox. γ-Al_2O_3 (100 m^2/g, Strem Chemicals) was pretreated by heating to 520 °C under flowing oxygen for 24 h, pumping off residual water for an additional 1 h at 520 °C, and finally cooling to room temperature under He flow. This treatment results in a partially dehydroxylated surface containing about 30% surface hydroxyl groups (σ-OH) and 35% surface oxide ions (σ-O^-) and having 35% oxide vacancies left (exposed Al^{3+} sites).[17] The pellets were stored under dry nitrogen in a Vacuum Atmospheres drybox equipped with a recirculating Dri-Train (Vacuum Atmospheres HE-493), which maintains an atmosphere of less than 1 ppm contaminants. H_2 (99.995%) and CO (99.99%) gases were obtained from Airco, and the tanks were fitted with Deoxo purifiers.

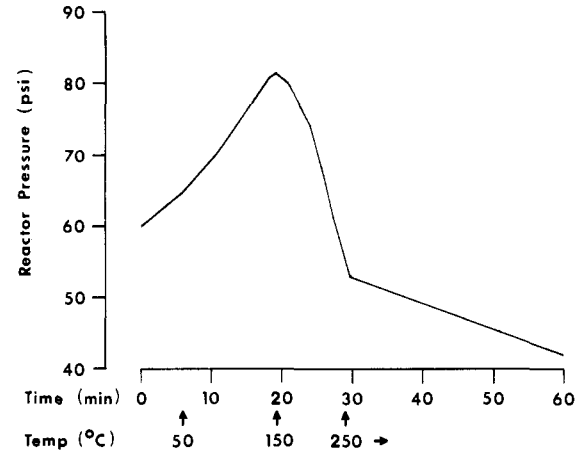

Figure 1. Reactor pressure vs. time of heating for $Co_4(CO)_{12}$–γ-Al_2O_3 under 3:2 H_2–CO. Apparent CO conversion begins at 150 °C.

Fischer–Tropsch (F-T) Reaction. Due to the pyrophoric nature of $Co_4(CO)_{12}$ all preparations and manipulations of the catalyst materials were carried out in the Vacuum Atmospheres drybox. In a typical F-T experiment, 200 mg (3.49×10^{-4} mol) $Co_4(CO)_{12}$ was dissolved in 100 mL of oxygen-free hexane. Five (5.00) grams of the partially dehydroxylated γ-Al_2O_3 was then added, and the solution was stirred. The reaction mixture, in a Pyrex insert, was then loaded into a 300-mL Parr minireactor (Parr Instrument Co.) equipped with a stirrer and heater. The following procedure was then adopted: The solvent was removed under vacuum for 1 h at room temperature.[18] The cluster was decarbonylated by heating under vacuum to 250 °C for an additional 1 h. After the reactor was allowed to cool to room temperature, the reactor was charged with 36 psi (2.5 atm) H_2 and 24 psi (1.6 atm) CO, corresponding to a 3:2 H_2–CO synthesis gas mixture and a total pressure of 60 psi (4.1 atm). The reactor was then heated, with stirring, to 250 °C for a specified length of time. Analysis of the gaseous products was obtained on a Perkin–Elmer Sigma 3 gas chromatograph (FID detector) using a 10-ft packed column of phenyl isocyanate on Porasil C and a linear temperature program, 40–80 °C, at 2 °C/min.

X-ray Photoelectron Spectroscopy (XPS). X-ray photoelectron spectra were recorded on a Hewlett-Packard 5950A ESCA spectrometer using a monochromatized Al Kα (1486.6-eV) source. The beam power was 800 W. For the XPS experiments, the alumina was pressed into pellets (suitable for mounting in the spectrometer) prior to impregnation with the hexane solution. Spectra of the Co 2p, O 1s, and Al 2s levels were obtained for catalyst samples after solvent evaporation, after decarbonylation, and after one F-T cycle. XPS spectra were recorded for three additional samples—one in which the hexane solution of $Co_4(CO)_{12}$ was allowed to evaporate onto the alumina support in the drybox, and two others in which the catalyst samples after one F-T cycle were subjected to moderate reduction (H_2, 30 psi, 250 °C, 4 h) and oxidation (O_2, 30 psi, 250 °C, 4 h)

(6) (a) Brenner, A.; Burwell, R. L. *J. Catal.* **1978**, *52*, 353. (b) Brenner, A.; Hucul, D. A. *Ibid.* **1980**, *61*, 216.
(7) (a) Anderson, J. R.; Elmes, P. S.; Howe, R. F.; Mainwaring, D. E. *J. Catal.* **1977**, *50*, 508. (b) Brenner, A. *J. Chem. Soc., Chem. Commun.* **1979**, 251. (c) Brenner, A.; Hucul, D. A. *Inorg. Chem.* **1979**, *18* (10), 2836.
(8) (a) Muetterties, E. L. *Catal. Rev.—Sci. Eng.* **1981**, *23* (1/2), 69. (b) Muetterties, E. L. *Bull. Soc. Chim. Belg.* **1976**, *85*, 451. (c) Thomas, M. G.; Beier, B. F.; Muetterties, E. L. *J. Am. Chem. Soc.* **1976**, *98*, 1296. (d) Demitras, G. C.; Muetterties, E. L. *Ibid.* **1977**, *99*, 2798.
(9) There is still some question as to the requirement of multinuclear sites in, for example, methanation: Brenner, A.; Hucul, D. A. *J. Am. Chem. Soc.* **1980**, *102*, 2484.
(10) (a) Muetterties, E. L. *Bull. Soc. Chim. Belg.* **1975**, *84*, 959. (b) Muetterties, E. L. *Science (Washington, D.C.)* **1977**, *196*, 839. (c) Muetterties, E. L.; Rhodin, T. N.; Band, E.; Brucker, C. F.; Pretzer, W. R. *Chem. Rev.* **1979**, *79*, 91.
(11) For a comprehensive review see: Bailey, D. C.; Langer, S. H. *Chem. Rev.* **1981**, *81*, 109 and references therein.
(12) (a) Commereuc, D.; Chauvin, Y.; Hughes, F.; Basset, J. M.; Oliver, D. *J. Chem. Soc., Chem. Commun.* **1980**, 154. (b) Schay, Z.; Guczi, L. *React. Kinet. Catal. Lett.* **1980**, *14*, 207. (c) Ballivet-Tkatchenko, D.; Coudrier, G.; Mozzanega, H.; Tkatchenko, I.; Kiennemann, A. *J. Mol. Catal.* **1979**, *6*, 293. (d) Ballivet-Tkatchenko, D.; Tkatchenko, I. *Ibid.* **1981**, *13*, 1. (e) Okuhara, T.; Kobayashi, K.; Kimura, T.; Misono, M.; Yoneda, Y. *J. Chem. Soc., Chem. Commun.* **1981**, 1114. (f) McVicker, G. B.; Vannice, M. A. *J. Catal.* **1980**, *63*, 25. (g) Deeba, M.; Scott, J. P.; Barth, R.; Gates, B. D. *Ibid.* **1981**, *71*, 373. (h) Blanchard, M.; Bonnet, R. *Bull. Soc. Chim. Fr.* **1977**, *1/2*, 7. (i) Lisitsyn, A. S.; Kuznetsov, V. L.; Yermakov, Y. I. *React. Kinet. Catal. Lett.* **1980**, *14*, 445. (j) Ichikawa, M.; Sekizawa, K.; Shikahura, K.; Kawai, M. *J. Mol. Catal.* **1981**, *11*, 167. (k) Ichikawa, M. *J. Chem. Soc., Chem. Commun.* **1978**, 566. (l) Ichikawa, M. *Bull. Chem. Soc. Jpn.* **1978**, *51*, 2268.
(13) (a) Hucul, D. A.; Brenner, A. *J. Am. Chem. Soc.* **1981**, *103*, 218. (b) Smith, A. K.; Theolier, A.; Basset, J. M.; Ugo, R.; Commereuc, D.; Chauvin, Y. *Ibid.* **1978**, *100*, 2591.
(14) (a) Cotton, G. A.; Jones, G. F. C.; Mays, M. J.; Howell, J. A. S. *Inorg. Chim. Acta* **1976**, *10*, L41. (b) Lennertz, A. M.; Laege, J.; Mirbach, M. J.; Sans, A. *J. Organomet. Chem.* **1979**, *171*, 203. (c) Ichakawa, M. *J. Catal.* **1979**, *56*, 127. (d) Ichakawa, M. *J. Catal.* **1979**, *59*, 67.
(15) Chini, P.; Albano, V.; Martinengo, S. *J. Organomet. Chem.* **1976**, *16*, 475.
(16) Noack, K. *Helv. Chim. Acta* **1962**, *45*, 1847.
(17) Peri, J. B. *J. Phys. Chem.* **1965**, *69* (1), 211.
(18) Typically, the volume of hexane recovered in the liquid-N_2 trap was 95% or better. The recovered solvent was clear, indicating no loss of the $Co_4(CO)_{12}$ cluster due to sublimation.

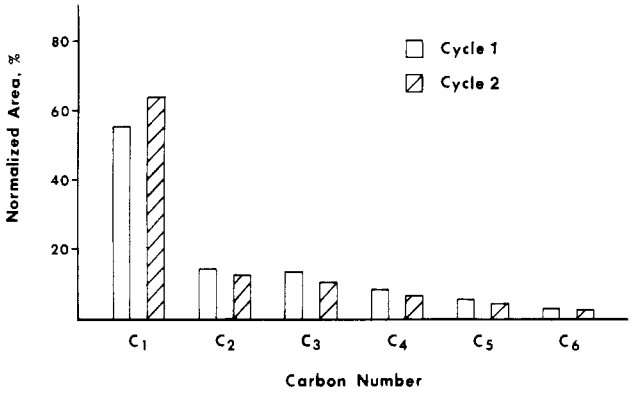

Figure 2. Hydrocarbon product distribution obtained for $Co_4(CO)_{12}$–γ-Al_2O_3 after two 4-h cycles at 250 °C under 3:2 H_2–CO.

treatments. Because of the insulating nature of the alumina, a low-energy flood gun was used to compensate for sample charging. All spectra were referenced to the Al 2s level set at 119.0 eV as an internal standard because it was felt that the aluminum was least sensitive to the above treatments. Spectral deconvolutions were obtained by a gaussian peak fit routine with linear background subtraction (Surface Science Laboratories, Inc.).

Laser-Induced Mass Spectroscopy (LIMS) and Transmission Electron Microscopy (TEM). The positive ion LIMS spectra were kindly provided by Dr. David M. Hercules of the University of Pittsburgh. In the LIMS experiment a pulsed laser source is used to flash vaporize a very small region (0.5–1 μm) of the catalyst surface and the fragments are analyzed by a mass spectrometer. As such, it is a *localized* surface technique and several LIMS spectra must be recorded to develop a consistent picture of the catalyst surface. Further, some caution must be exercised in the absolute interpretation of the results owing to fragmentation and/or sintering of surface species caused by the LIMS experiment itself. In the absence of standardization of the technique, we can only have faith in the relative differences observed when the catalyst is subjected to various treatments. The TEM of all catalyst samples was performed with a Hitachi Model HU-11E-1 electron microscope housed in the Electron Microscopy Center at Texas A&M University. These latter samples were prepared by coarse grinding of the catalyst under dry nitrogen prior to depositing in the epoxy resin.

Results

A plot of the total pressure (psi) vs. time of heating (temperature) for a typical F-T cycle is shown in Figure 1. Initially the pressure rises linearly with temperature until about 150 °C, where it drops precipitously as the apparent conversion of CO begins. Analysis of the gaseous contents of the Parr bomb (Figure 2) shows a typical Fischer–Tropsch distribution of low-molecular-weight hydrocarbons. No attempt was made to resolve the C_4 and higher hydrocarbons into isomeric and/or olefinic contributions (although the C_4, C_5, and C_6 regions had two components each). These additional components are probably branched isomers as conventional Co-based F-T catalysts are known to produce linear and branched alkanes.[4]

We established that the reaction was catalyzed by $Co_4(CO)_{12}$ by the following experiments. The system was recycled with a fresh charge of H_2–CO with similar results (Figure 2). If, after one F-T cycle, the catalyst was charged with H_2 *alone* (36 psi, 250 °C, 4 h), a moderate amount of CH_4 was detected and only trace amounts of C_2–C_5 hydrocarbons were present. If this system was then charged with CO (60 psi, 250 °C, 4 h), there were no detectable hydrocarbons present. An attempt to synthesize hydrocarbons following the usual procedure in the absence of $Co_4(CO)_{12}$ failed.

The XPS spectra of the Co 2p levels for the catalyst taken at various stages and subjected to various treatments are shown in Figure 3. The assignment of cobalt oxidation states is most readily accomplished by examination of the satellite structure of the $2p_{3/2}$ level and also by consideration of the spin–orbit splitting of the 2p levels[19] (Table I). Typically, one or more

Table I. Spin–Orbit Splittings and Satellite Line Separations

	ΔE_{s-o}[a]				
	oxidized	metallic	Co $2p_{3/2}$ satellites[a]		% metallic
treatment	Co	Co	I	II	Co
solvent evac	16.2		3.9 (0.69)	8.7 (0.64)	
decarbonylated	15.7	14.7	4.7 (1.45)		18
F-T reacn	16.0	14.0	4.9 (0.95)		22
O_2	15.2		6.2 (0.85)		
Petri evap	15.8		4.1 (0.83)	7.6 (0.68)	
H_2	16.2	15.1	5.8 (0.95)		25

[a] All values are in eV. Quantities in parentheses are the relative intensities of the satellite to the $2p_{3/2}$ level.

intense satellites may appear at 4–7 eV above the $2p_{3/2}$ level in high-spin Co(II) complexes, and the spin–orbit splitting is ~16.0 eV. Low-spin Co(III) complexes show only weak satellites at 8–9 eV above the $2p_{3/2}$ level, and the spin–orbit splitting is ~15.0 eV. The 2p levels in Co metal show no satellite structure, and the spin–orbit splitting is 15.0 eV.[20] Chemical shift data are less reliable because of the overlap in the $2p_{3/2}$ positions for Co(II) high-spin and Co(III) low-spin complexes.[19c] The binding energies of the Co 2p, O 1s, and Al 2s levels are shown in Table II.

Qualitative analysis of the spectra in Figure 3 (and data from Tables I and II) suggests the following: Figure 3a shows the catalyst after the solvent has been removed under vacuum from the reactor at room temperature. This material is brownish purple and will turn a pale blue after 1 h under dry nitrogen. By way of comparison, a more concentrated solution of $Co_4(CO)_{12}$ in hexane was allowed to evaporate onto the alumina support in the drybox (Figure 3e). This material was found to undergo a similar color change although the resulting material was a deeper blue. The spectra shown in parts a and e of Figure 3 are of the blue material. Both of these samples have Co 2p levels exhibiting two intense satellites (Table I). The spin–orbit splitting of the vacuum-evaporated sample is 16.2 eV while that of the drybox sample is 15.8 eV (Table I). Although the Co $2p_{3/2}$ binding energy is about 1 eV lower for the vacuum-evaporated sample (Table II), the intensity of the satellites and large spin–orbit splitting suggests that Co(II) is present.

Figure 3b shows the Co 2p region after thermal decarbonylation. This material is black-grey. Since this thermal decarbonylation was carried out immediately after solvent evacuation at room temperature, the presence of metallic cobalt is readily seen as a low-binding-energy shoulder at 778.6 eV on the Co $2p_{3/2}$ peak of the oxidized cobalt at 781.7 eV (Table II). Deconvolution of the spectrum reveals that the extent of metallic cobalt present is 18%. The 2p levels of the oxidized component have one intense satellite each and are split by 15.7 eV, suggesting that the oxidized cobalt is present as Co(II) (Table I). The splitting of the 2p levels in the metallic cobalt, 14.7 eV, is less certain due to the fact that the $2p_{1/2}$ component is somewhat obscured by the more intense oxidized cobalt bands.

Figure 3c shows the Co 2p levels of the catalyst after one F-T cycle. This spectrum looks similar to that of the decarbonylated sample (Figure 3b); however, the contribution due to metallic cobalt has increased to 22%. The spin–orbit splitting of the metallic component, 14.0 eV (Table I), is low due mostly to the uncertainty in the position of the $2p_{1/2}$ level, 792.5 eV, which is again obscured. The oxidized cobalt exhibits 2p levels that are split by 16.0 eV, and each exhibits

(19) (a) Frost, C. D.; McDowell, C. A.; Woolsey, I. S. *Chem. Phys. Lett.* **1972**, *17* (3), 320. (b) Frost, C. D.; McDowell, C. A.; Woolsey, I. S. *Mol. Phys.* **1974**, *27* (6), 1473. (c) Okamoto, Y.; Nakano, H.; Imanaka, T.; Teranishi, S. *Bull. Chem. Soc. Jpn.* **1975**, *48* (4), 1163.
(20) Brundle, C. R.; Chaung, T. J.; Rice, D. W. *Surf. Sci.* **1976**, *60*, 286.

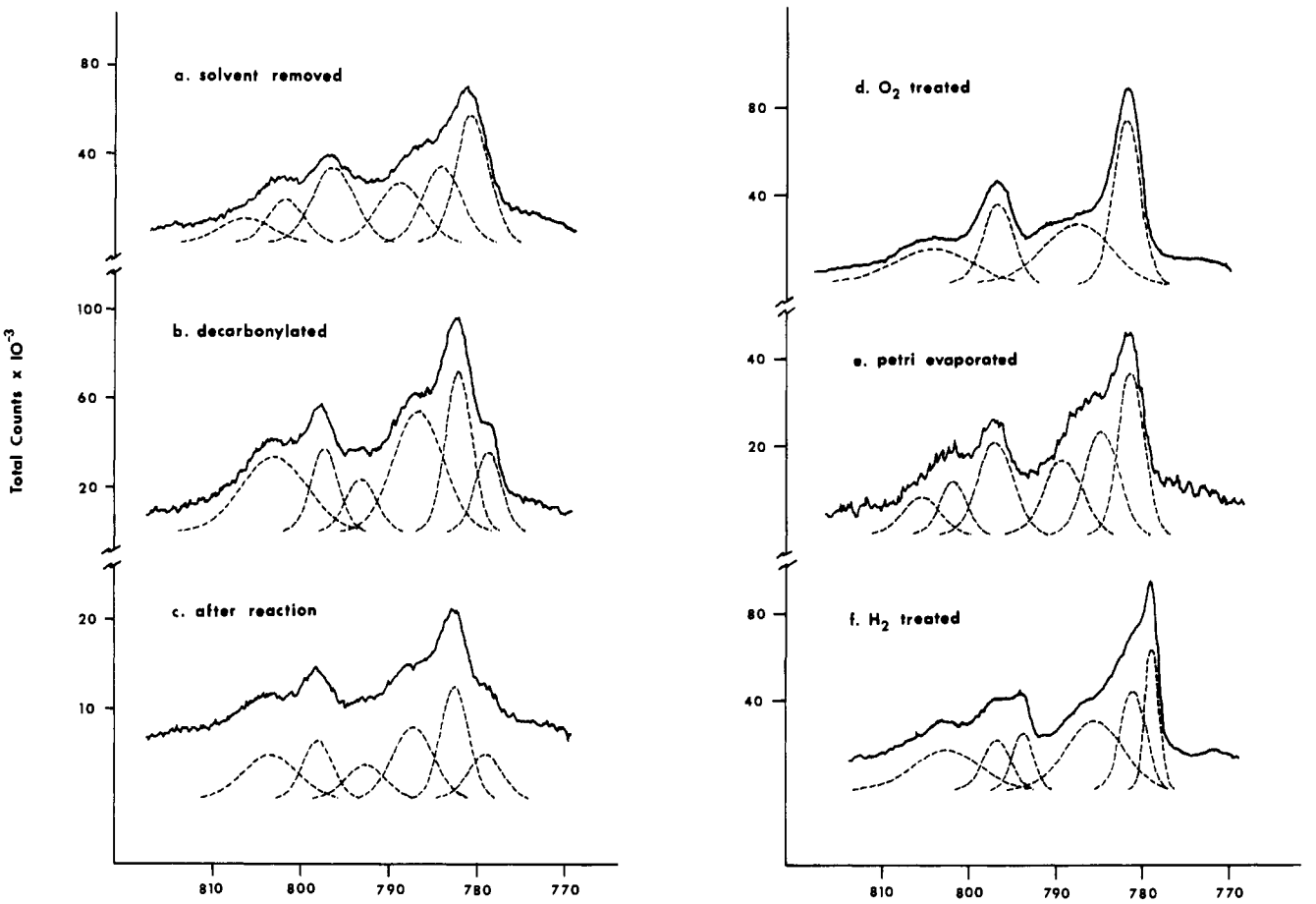

Figure 3. Co 2p XPS spectra of $Co_4(CO)_{12}$–γ-Al_2O_3: (a) after solvent removal in vacuo at room temperature; (b) after thermal decarbonylation in vacuo to 250 °C; (c) after one F-T cycle under 3:2 H_2–CO at 250 °C; (d) after one F-T cycle and after moderate oxidation (O_2, 30 psi, 250 °C); (e) after solvent evaporation of $Co_4(CO)_{12}$–hexane onto γ-Al_2O_3 at room temperature; (f) after one F-T cycle and after moderate reduction (H_2, 30 psi, 250 °C). Spectral deconvolutions are indicated by dashed lines.

Table II. Binding Energies[a] and Half-Widths

	oxidized Co		metallic Co			
treatment	$2p_{1/2}$	$2p_{3/2}$	$2p_{1/2}$	$2p_{3/2}$	O 1s	Al 2s
solvent evac	797.3 (5.8)	781.1 (4.5)			531.3 (2.9)	119.0 (2.7)
decarbonylated	797.4 (3.6)	781.7 (3.5)	793.3 (4.2)[b]	778.6 (3.6)[b]	531.3 (2.9)	119.0 (3.0)
F-T reacn	797.9 (4.0)	782.0 (3.7)	792.5 (5.4)[b]	778.5 (4.8)[b]	531.3 (3.0)	119.0 (3.0)
O_2	796.0 (4.2)	780.8 (3.8)			531.3 (2.9)	119.0 (2.7)
Petri evap	797.9 (4.9)	782.1 (3.5)			531.1 (2.8)	119.0 (2.9)
H_2	797.3 (4.2)	781.1 (3.8)[b]	794.5 (2.9)	779.4 (1.9)	532.1 (2.5)	119.0 (3.0)
					530.2 (1.9)	116.7 (3.2)
					528.7 (2.1)	

[a] Reported binding energies are in eV and are considered reliable to within ±0.2 eV. [b] Binding energies are less certain due to masking or shoulders.

a strong satellite, which suggests that Co(II) is present (Table I). That the overall intensity of the 2p region has diminished relative to those in Figure 3a,b is most likely due to a diminished cobalt concentration on this particular sample.

Figure 3d shows the Co 2p region of a sample after one F-T cycle and after moderate oxidation treatment (O_2, 30 psi, 250 °C). This material is olive green. This treatment has resulted in the disappearance of metallic cobalt from the surface of the catalyst. The $2p_{3/2}$ binding energy of the oxidized cobalt has shifted to the lowest value seen on any sample, 780.8 eV (Table II). Although the 2p levels are split by 15.2 eV, each level exhibits a moderately intense satellite, suggesting that complete oxidation of Co(II) to Co(III) has not occurred.

Figure 3f shows the catalyst after one F-T cycle and after moderate reduction treatment (H_2, 30 psi, 250 °C). This material is black with some visible mirroring. The most intense lines are due to reduced cobalt appearing at lower binding energy. The $2p_{3/2}$ binding energy of reduced cobalt is 779.4 eV (Table II). Deconvolution of the spectrum reveals that reduced cobalt accounts for 25% of the cobalt species present. The intensity due to metallic cobalt appears even greater on the reduced sample than on the decarbonylated (Figure 3b) or post F-T reaction (Figure 3c) samples because of the significantly narrower half-width, 1.9 eV, of the $2p_{3/2}$ level in the first sample (compare in Table II). The 2p levels of the oxidized component are split by 16.2 eV, and each exhibits one intense satellite, suggesting that Co(II) is present. The absolute value of this splitting is considered to be less certain because the $2p_{3/2}$ level appears as a higher binding energy shoulder on the metal peak at 781.1 eV (Table II).

While all other samples exhibited one line in both the O 1s and Al 2s regions of comparable binding energy and half-width, the reduced sample exhibited some splitting in both these regions (see Table II). Thus, the O 1s exhibited three ionizations at 532.1, 530.2, and a low-binding-energy shoulder at 528.7 eV (Table II). The Al 2s region exhibited a relatively

Table III. Positive Ion LIMS

treatment	positive ions due to	intens[c]
decarbonylation, 250 °C, 1 h[a]	Co^+	s
	Co_x^+ (x = 2, 5, 6, 7)	w
F-T reacn, 250 °C, 2 h[b]	Co^+	s
	$Co_4(CO)_x^+$ (x = 2–6)	w
	$Co_4(CO)_xC^+$ (x = 0, 1, 2, 4, 11)	w
	$Co_4(CO)_xCH_2^+$ (x = 4)	w

[a] Results of 5 spectra. [b] Results of 13 spectra. [c] Key: s, strong; w, weak.

strong ionization at 116.7 eV with a lower intensity shoulder toward higher binding energy at 119.0 eV (Table II).

Positive ion LIMS data of two samples are presented in Table III. The first was of the catalyst after thermal decarbonylation but before the F-T reaction. The second was of the active catalyst after one F-T cycle. The decarbonylated sample shows a strong mass peak due to individual cobalt atoms or ions and weaker mass peaks due to clusters of Co_2, Co_5, Co_6, and Co_7. The active catalyst after one F-T cycle is substantially different. In addition to the strong mass peaks due to individual cobalt atoms or ions, only clusters of Co_4 are observed with varying numbers of CO ligands, $Co_4(CO)_x^+$ (Table III). Still more intriguing is the appearance of mass peaks that can only be explained by $Co_4(CO)_x$ clusters containing a bare carbon atom, $Co_4(CO)_xC^+$, and, in one case, a methylene unit, $Co_4(CO)_4CH_2^+$ (Table III).

Transition electron micrographs of all catalyzed samples during pretreatment, the F-T cycle, and postreaction treatments revealed no visible cobalt clusters at magnification ×258 000 (i.e. no clusters greater than 10-nm diameter).

Discussion

It is known that the molecular weight distribution of products observed in the F-T reaction may be treated mathematically as a polymerization process.[21] A typical distribution of products after one F-T cycle of the $Co_4(CO)_{12}$–γ-Al_2O_3 system is shown in Figure 4 (data from cycle 1, Figure 2) following the Flory polymerization equation[21b]

$$\ln m_n = \ln \alpha\, C_n + \ln\left(\frac{1-\alpha}{\alpha}\right) \qquad (1)$$

where m_n is the mole fraction of total hydrocarbons produced, C_n is the number of carbon atoms in the polymer chain, and α is the chain propagation factor (rate of propagation/(rate of propagation + rate of termination)). That α appears in both the slope and intercept provides an independent check, and the average of these two values is usually reported.

After one F-T cycle (250 °C, 4 h), the average value of α is 0.47 ± 0.06 (Figure 4). Assuming 100% dispersion of the catalyst, the turnover number is 4.4 mmol of C/mmol of Co at an experimental conversion of 51% (for hydrocarbon) or 70% (for hydrocarbon plus theoretical CO_2).[22] If the catalyst is used in a second F-T cycle (250 °C, 4 h), the average value of α is essentially unchanged at 0.47 ± 0.08 (data from cycle 2, Figure 2). If, instead, the second cycle is done under H_2 *alone* (36 psi, 250 °C, 4 h), moderate amounts of CH_4 and only trace amounts of C_2–C_5 hydrocarbons are produced. In this case the apparent conversion of CO begins at or near 250 °C. Further, the product distribution after this H_2 treatment is not amenable to treatment by the Flory equation, (1). We will comment further on these observations later.

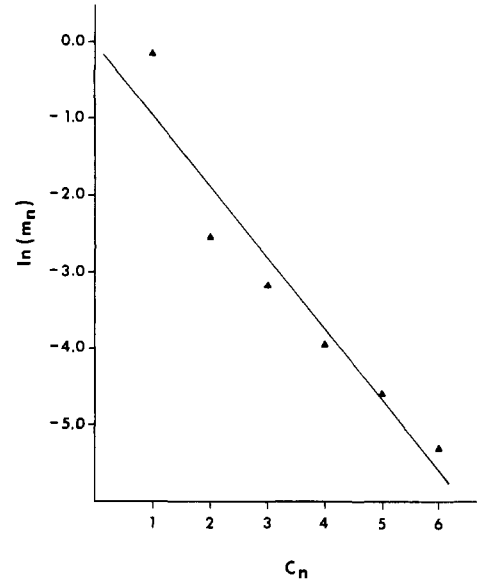

Figure 4. Flory representation of C_1–C_6 hydrocarbon products after one F-T cycle (data from cycle 1, Figure 2).

Room-Temperature Solvent Evaporation. After initial physisorption, the interaction of metal carbonyls with an alumina support is likely to involve some substitution of the CO ligands by a basic surface oxy group (surface hydroxyl, σ-OH, a surface oxide, σ-O^-, or both) to form adsorbed subcarbonyls.[23a] Another mode of interaction is likely to involve coordination of the oxygen atom of the CO ligand with exposed Lewis acid sites (Al^{3+}) on the alumina.[23] Bjorklund and Burwell observed a yellow intermediate when $Ni(CO)_4$ was deposited on partially dehydroxylated γ-Al_2O_3 at 23 °C, which was attributed to the formation of $Ni(CO)_3$(ads).[24a] Slightly higher temperatures are required to form the stable $Mo(CO)_3$(ads)[6a,24b] and $W(CO)_3$(ads)[6b] from $Mo(CO)_6$ and $W(CO)_6$ (although a yellow intermediate presumed to be $Mo(CO)_5$(ads) was observed at room temperature[6a,25]). Further, these subcarbonyls give back the parent carbonyl under CO treatment.[6b,24a,b]

The hexane solution of $Co_4(CO)_2$ and γ-Al_2O_3 is a deep brown-black. Removal of the hexane results in a brownish purple material that is extremely sensitive to oxidation and will turn to a pale blue in the Vacuum Atmospheres drybox within 1 h. It is likely that the brownish purple material is a subcarbonyl, $Co_4(CO)_x$(ads), of $Co_4(CO)_{12}$ and that additional interaction of surface oxy groups (or trace amounts of atmospheric oxygen or water vapor) causes a rapid oxidation to give the pale blue material. Laniecki and Burwell[25] have proposed the formation of surface carbonate or bicarbonate species when the concentration of surface oxide groups is high as on partially or completely dehydroxylated γ-Al_2O_3. Our γ-Al_2O_3 pretreatment results in a surface containing about 65% basic sites (~30% σ-OH, ~35% σ-O^-).[17]

The XPS spectra of the pale blue material (Figure 3b,e) show only the presence of Co(II). Room-temperature interaction of $Co_4(CO)_{12}$ with alumina results in oxidation of the cobalt relative to the parent cluster. This result is not surprising in view of the pyrophoric nature of $Co_4(CO)_{12}$, which

(21) (a) Henrici-Olive, G.; Olive, S. *Angew. Chem., Int. Ed. Engl.* **1976**, *15*, 136. (b) Satterfield, C. N.; Huff, G. A. *J. Catal.* **1982**, *73*, 187. (c) Flory, P. J. *J. Am. Chem. Soc.* **1936**, *58*, 1877.

(22) By way of comparison, a catalyst prepared in an identical manner with use of $Co_2(CO)_8$ at the same metal loading gave a similar value of α = 0.49 ± 0.05 after one F-T cycle; however, the turnover number was significantly smaller, 2.9 mmol of C/mmol of Co, at a lower experimental conversion of 40% (for hydrocarbons).

(23) (a) Brown, T. L. *J. Mol. Catal.* **1981**, *12*, 41 and references therein. (b) Kristoff, J. S.; Shriver, D. F. *Inorg. Chem.* **1974**, *13* (3), 499. (c) Shriver, D. F. *J. Organomet. Chem.* **1975**, *94*, 259. (d) Howe, R. F.; Kazusaka, A. *J. Mol. Catal.* **1980**, *9*, 183.

(24) (a) Bjorklund, R. B.; Burwell, R. L. *J. Colloid Interface Sci.* **1979**, *70* (2), 383. (b) Brenner, A.; Burwell, R. L. *J. Am. Chem. Soc.* **1975**, *97* (9), 2565. (c) Burwell, R. L.; Brenner, A. *J. Mol. Catal.* **1975/76**, *1*, 77.

(25) Laniecki, M.; Burwell, R. L. *J. Colloid Interface Sci.* **1980**, *75*(1), 95.

decomposes at 60 °C.[26a] Lisitsyn et al.[12i] observed a marked change in the ν_{CO} region when $Co_2(CO)_8$ (decomposition temperature, 51 °C[26b]) was deposited on γ-Al_2O_3 (precalcined at 600 °C) at room temperature. This was attributed to decomposition of the carbonyl by hydrolysis of σ-OH groups. It is difficult to say whether this oxidation has resulted in the partial or complete decomposition of the tetracobalt cluster at this point. The color change, from brownish purple to pale blue, does suggest a change in coordination number about the cobalt has occurred. In the initial cluster, zerovalent cobalt is six-coordinate at the apical Co atom and seven-coordinate in the basal Co atoms.[27] The color change to pale blue with concomitant oxidation of the metal does suggest that the Co(II) species are tetrahedrally coordinated.[28]

Thermal Decarbonylation. If thermal decarbonylation to 250 °C under vacuum is allowed to proceed immediately after solvent removal, a catalyst material that is black-grey results. In addition to oxidized Co(II) species, the XPS of this sample (Figure 3b) shows the presence of metallic cobalt (18%). This thermal treatment has retarded complete oxidation of Co(0) to Co(II). The LIMS data shows that complete decarbonylation has occurred. This is consistent with the IR studies of Psaro et al.,[29] who monitored the disappearance of ν_{CO} when $Co_4(CO)_{12}$ was heated to 250 °C in a KBr matrix. Thermogravimetric data by the same authors indicate that decarbonylation of unsupported $Co_4(CO)_{12}$ to cobalt metal is complete at 170 °C at a heating rate of 10 °C/min, while some oxidation of the metal occurs when the heating rate was 1 °C/min.[29] Our thermal decarbonylation is carried out at a rate of about 4 °C/min. The oxidation of cobalt under thermal treatment in the case of supported $Co_4(CO)_{12}$ is likely due to a redox reaction involving interaction of σ-OH groups from the support.[6a,7b,c,30]

In addition, the LIMS data (Table III) indicate that the original Co_4 cluster has fragmented into individual cobalt atoms or ions and, to a lesser extent, reorganized into clusters of various sizes producing Co_2, Co_5, Co_6, and Co_7 species. In contrast, the mass spectrum of unsupported $Co_4(CO)_{12}$ by Johnson et al.[31] has shown fragmentation involves loss of all the CO ligands (i.e., the ions $Co_4(CO)_{12-x}^+$, where x = 0–12, are observed) with retention of the Co_4 nucleus. Ions due to Co^+, Co_2^+, and Co_3^+ were also observed. Pyrolysis of unsupported $Co_4(CO)_{12}$ in sealed, evacuated tubes from 63 to 100 °C results in the formation of $Co_6(CO)_{16}$.[32] Clearly, thermal decarbonylation of $Co_4(CO)_{12}$ on partially dehydroxylated γ-Al_2O_3 results in the stabilization of a variety of cobalt species that are not available to the unsupported cluster under similar treatments. That these species are highly dispersed is confirmed by the lack of visible cobalt particles in the TEM.

Fischer–Tropsch (F-T) Reaction. Heating the decarbonylated catalyst material under a 3:2 H_2–CO mixture to 250 °C produces no visible change in the catalyst color. The XPS (Figure 3c) reveals that the percent of metallic cobalt species has increased slightly to 22% (Table I). This slight increase in reduced cobalt species under the reducing conditions of the F-T reaction would suggest that the Co(II) present after thermal decarbonylation was tetrahedrally coordinated, as tetrahedrally coordinated Co(II) is more resistant to reduction than octahedrally coordinated Co(II).[33]

In addition to individual cobalt atoms or ions, the LIMS data reveal that only clusters of Co_4 are observed with various numbers of CO ligands (Table III). It would seem that the most stable arrangement of cobalt under reaction conditions is that of the original cluster, i.e. Co_4 units. The odd size clusters observed after thermal decarbonylation must be in close enough proximity to reorganize to form the more stable four atom units. These units are partially recarbonylated with the remaining coordination sites presumably occupied by direct bonding with the support. Perhaps more exciting is the observation of cluster carbido carbonyls, $Co_4(CO)_xC$, where x = 0,1,2,4,11, and, in one case, a cluster methylene unit, $Co_4(CO)_4CH_2$ (Table III). We have already noted that pyrolysis of the unsupported $Co_4(CO)_{12}$ does not result in carbide formation.[32] Since no carbides were present after thermal decarbonylation, carbon atom incorporation must be occurring under F-T conditions.

The original mechanism by Fischer and Tropsch in 1926[34] proposed that hydrocarbon formation under CO and H_2 on certain transition metals proceeded by polymerization of methylene units on the metal surface. Although other mechanisms[35] have since been proposed, more recently, Brady and Pettit[36] have provided strong evidence that the original Fischer–Tropsch mechanism (dubbed the carbide mechanism) correctly accounts for hydrocarbon production in the F-T synthesis. In particular, these authors found that, in the presence of H_2, methylene units derived from CH_2N_2 do polymerize on Fe, Co, and Ru surfaces to give hydrocarbon product distributions consistent only with the Fischer–Tropsch scheme.[36a] They proposed that with H_2–CO reactant mixtures methylene units may be produced from reduction of metal carbides produced by dissociative CO adsorption. Reduction of a methylene unit to a methyl group and subsequent insertion of methylene units would account for propagation of the hydrocarbon chain. Further support was added to the carbide mechanism when it was discovered that if an additional source of methylene units (in the form of CH_2N_2) was added to a H_2–CO feed over a Co–Kiesulguhr catalyst, the rate of chain propagation (to termination) increased by a factor of 3.3 over the reaction in the absence of added CH_2N_2.[36b]

The observation that only a moderate amount of CH_4 and trace amounts of C_2–C_5 hydrocarbons are observed after a second cycle of H_2 *alone* could be explained in two ways. First, these products may be due to hydrogenation or residual cluster carbide or cluster methylene units. It is known that "carbidic" carbon derived from dissociative adsorption of CO on unsupported[37a] and supported[37b–e] F-T metals will hydrogenate to methane at moderate temperatures. These studies,[37b,c]

(26) Hagihara, N. Kumada, M. Okawara, R., Eds. "Handbook of Organometallic Compounds"; W. A. Benjamin: New York, 1968: (a) p 859. (b) p 856.
(27) (a) Wei, C. H.; Dahl, L. F. *J. Am. Chem. Soc.* **1966**, *88*, 1821. (b) Carre, F. H.; Cotton, F. A.; Frenz, B. A. *Inorg. Chem.* **1976**, *15* (2), 380.
(28) Cotton, F. A.; Wilkinson, G. "Advanced Inorganic Chemistry", 3rd ed.; Interscience: New York, 1972; p 880.
(29) Psaro, R.; Fusi, A.; Ugo, R.; Basset, J. M.; Smith, A. K.; Hughes, F. *J. Mol. Catal.* **1980**, *7*, 511.
(30) (a) Brenner, A.; Hucul, D. A. *J. Phys. Chem.* **1981**, *85*, 496. (b) Brenner, A.; Hucul, D. A. *Prepr., Div. Pet. Chem., Am. Chem. Soc.* **1977**, *22*, 1221. (c) Brenner, A.; Hucul, D. A.; Hardwick, S. J. *Inorg. Chem.* **1979**, *18* (6), 1478.
(31) Johnson, B. F. G.; Lewis, J.; Williams, I. G.; Wilson, J. M. *J. Chem. Soc. A* **1967**, 341.
(32) Eady, C. R.; Johnson, B. F. G.; Lewis, J. *J. Chem. Soc., Dalton Trans.* **1975**, 2606.
(33) (a) Chin, R. L.; Hercules, D. M. *J. Phys. Chem.* **1982**, *86*, 360. (b) DeClerck-Grimee, R. I.; Canesson, P.; Friedman, R. M.; Fripiat, J. J. *Ibid.* **1978**, *82*, 885. (c) Chung, K. S.; Massoth, F. E. *J. Catal.* **1980**, *64*, 320.
(34) (a) Fischer, F.; Tropsch, H. *Brennst.-Chem.* **1926**, *7*, 97. (b) Fischer, F.; Tropsch, H. *Chem. Ber.* **1926**, *59*, 830.
(35) (a) Rofer-Depoorter, C. K. *Chem. Rev.* **1981**, *81*, 447 and references therein. (b) Bell, A. T. *Catal. Rev—Sci. Eng.* **1981**, *23* (1/2), 203 and references therein.
(36) (a) Brady, R. C.; Pettit, R. *J. Am. Chem. Soc.* **1980**, *102*, 6182. (b) Brady, R. C.; Pettit, R. *Ibid.* **1981**, *103*, 1287.
(37) (a) Bonzel, H. P.; Krebs, H. J. *Surf. Sci.* **1982**, *117*, 639. (b) Rabo, J. A.; Risch, A. P.; Poutsma, M. L. *J. Catal.* **1978**, *53*, 295. (c) Low, G. G.; Bell, A. T. *Ibid.* **1979**, *57*, 397. (d) Wentrcek, P. R.; Wood, B. J.; Wise, H. *Ibid.* **1976**, *43*, 363. (e) Biloen, P.; Helle, J. N.; Sachtler, W. J. M. *Ibid.* **1979**, *58*, 95.

including ^{13}C tracer studies,[37e] have shown that higher homologues of methane may be formed. More pertinent to our case is the finding by Muetterties et al. that the reactivity of carbidic carbon atoms increases as the coordination number of the carbide atom decreases.[38] Thus, the μ_5-C carbon of $Fe_5C(CO)_{15}$ is not reactive up to 80 °C, where the cluster decomposes,[38a] while the μ_4-C carbon of $Fe_4C(CO)_{12}^{2-}$ can be hydrogenated to $HFe_4(\eta^2\text{-}CH)(CO)_{12}$ by oxidation with Ag^+ in the presence of H_2 at 25 °C.[38b,c] In addition, Shriver et al. have demonstrated the unique ability of M_4 (as opposed to M_2 or M_3) carbonyl clusters to undergo H^+-induced CO reduction to CH_4 in solution, presumably via M_4C intermediates.[39] It is very likely that carbide carbon in residual Co_4C units could be hydrogenated to form the observed products after a second cycle under H_2 *alone*. The source of the carbide carbon would probably derive from CO disproportaionation (according to the Boudouard reaction, $2CO = CO_2 + C_s$). Although our GC detector (FID) is not sensitive to CO_2, we found that the amount of CO_2 present after one F-T cycle was comparable to that of CH_4 by GC–MS analysis of one sample. We are currently exploring the role of "carbidic" carbon in the F-T reaction by supporting alkylidyne clusters.

A second contributing factor to the observed products after a second H_2 cycle could be the stoichiometric reduction of coordinated CO. Hucul and Brenner[9,13a] have observed CH_4 formation (and trace amounts of C_2H_6, C_2H_4) in the temperature-programmed decomposition of $Co_4(CO)_{12}$ on partially dehydroxylated γ-Al_2O_3 under flowing H_2 at 150 °C. The presence of these hydrocarbons was attributed to the reduction of coordinated CO on subcarbonyl species stabilized on the support. In these studies, only trace amounts of CO_2 were evolved and so hydrogenation of surface carbon was not considered responsible. Our LIMS data shows that subcarbonyls of formula $Co_4(CO)_x$ (Table III) are present after one F-T cycle and that reduction of coordinated CO may be possible as well.

In any case, the product distributions obtained from the two cycles under H_2–CO are consistent with a polymerization scheme involving addition of methylene units one at a time and reconcilable with the proposed mechanism of Fischer and Tropsch. The distribution of products observed after the second cycle under H_2 *alone* is not reconcilable with such a scheme, and hydrocarbon production, in this latter case, does not appear to involve additional chain growth.

Postreaction Treatments: Reduction and Oxidation. Moderate reduction (H_2, 30 psi, 250 °C) of the catalyst after one F-T cycle results in a black, heterogeneously mirrored material. The XPS of the Co 2p region (Figure 3f, Tables I and II) reveals that the contribution of reduced cobalt has increased to 25% (a 3% increase over that one F-T cycle). That the intensity of the photoemission from this reduced cobalt dominates the spectrum in this sample is due to the significantly narrower half-width, 1.9 eV, compared to that of other samples where metallic cobalt appears: 3.6 eV (after decarbonylation) and 4.8 eV (after one F-T cycle) (Table I). The slight increase in reducibility suggests tetrahedral coordination of Co(II) ions present after one F-T cycle as has already been noted.[33]

Some mention of the state of reduced cobalt species present in these samples should be made. In no case do the binding energies of the reduced cobalt approach that of the bulk metal. Brundle et al.[20] have reported that the $2p_{3/2}$ level of an electron-beam deposited, argon-etched cobalt film occurs at 778.2 eV with a half-width of 1.3 eV. Others have reported still lower values for the $2p_{3/2}$ binding energy of 778.0[40] and 777.8 eV,[19c] the slight discrepency presumably due to differences in binding energy calibration. The metallic cobalt peaks appearing in the decarbonylated, postreaction, and reduced samples occur at 778.6 (shoulder), 778.5 (shoulder), and 779.4 eV, respectively (Table II). It is known that core levels for small metal particles shift to higher binding energies as the particle size decreases due to diminished electron screening.[41] Only a moderate shift is observed on the decarbonylated and postreaction samples, where the LIMS confirm the presence of small cobalt clusters. The much larger shift of 1.2 eV relative to that for the bulk for the hydrogen-treated sample and the absence of visible cobalt particles in the TEM suggest that highly dispersed Co metal is formed. The spin–orbit splitting, 15.1 eV (Table I), is similar to that of the bulk metal. Similar conclusions have been drawn from the XPS data of $Rh_6(CO)_{16}$–γ-Al_2O_3 under high-temperature treatments, which are known to fragment the cluster.[42]

In addition, the postreaction reduction treatment gives rise to splitting in the O 1s and Al 2s regions. The O 1s region exhibits three ionizations of decreasing intensity at 532.1, 530.1, and 528.7 (shoulder) eV (Table II). We tentatively assign these bands as follows: The intense band at 532.1 eV is due to hydrogen-bonded oxygen, perhaps surface hydroxyl groups or adsorbed H_2O. The medium-intensity band at 530.2 eV is due to surface oxide (σ-O^-), and the lower intensity shoulder at 528.7 eV is due to oxygen bound to an electropositive metal impurity in the support.

Wagner et al.[43] have demonstrated the importance of combining Auger spectroscopy with XPS to determine the surface chemical state of oxygen in a variety of organic and inorganic compounds. In the absence of Auger data, the above assignments are at best tentative; however, the binding energies fall in or near the regions reported by Wagner (H_2O (solid) 532.9 eV, aluminas 531.1–531.9 eV, and metal oxides 529.4–530.1 eV). All other catalyst samples exhibit only one O 1s line of similar binding energy and half-width (Table II), which lies intermediate between the first two observed in the reduced sample. If one assumes that the O 1s XPS in all other samples is characteristic of the oxygen species in partially dehydroxylated γ-Al_2O_3, then hydrogen treatment has resulted in the reduction of some surface oxy species to adsorbed H_2O (532.1 eV) and left some surface oxy species (presumably σ-O^-, not σ-OH) unaffected (530.2 eV). The low-binding-energy shoulder at 528.7 eV is likely due to the presence of alkali-metal oxides, which are present in the support. Positive ion LIMS data of the pretreated γ-Al_2O_3 alone show trace amounts of Li^+ and Na^+ ions. After thermal decarbonylation only trace amounts of Li^+ are seen. After one F-T cycle, however, moderate amounts of Li^+, Na^+, and K^+ are seen. In one case, the relative abundance of Na^+–Al^+ was 0.86. Prolonged 250 °C treatments of the catalyst may result in segregation of these impurities to the catalyst surface.

The hydrogen treatment also gives rise to splitting in the Al 2s region. Two ionizations are observed, a high-binding-energy shoulder, at 119.0 eV, to the more intense 116.7 eV peak. These two ionizations are due to Al^{3+} in different insulating domains. Overcharging is likely to be observed on the reduced sample for the following reasons: (1) the flood

(38) (a) Muetterties, E. L.; Stein, J. *Chem. Rev.* **1979**, *79* (6), 479. (b) Tachikawa, M.; Muetterties, E. L. *J. Am. Chem. Soc.* **1980**, *102*, 4541. (c) Beno, M. A.; Williams, J. M.; Tachikawa, M.; Muetterties, E. L. *Ibid.* **1980**, *102*, 4542.

(39) Drezdon, M. A.; Whitmire, K. H.; Bhattacharyya, A. A.; Hsu, W.-L.; Nagel, C. C.; Shore, S. G.; Shriver, D. F. *J. Am. Chem. Soc.* **1982**, *104*, 5630.

(40) McIntyre, N. S.; Cook, M. G. *Anal. Chem.* **1975**, *47* (13), 2208.

(41) (a) Takasu, Y.; Unwin, R.; Tesche, B.; Bradshaw, A. M. *Surf. Sci.* **1978**, *77*, 219. (b) Apai, G.; Lee, S.-T.; Mason, M. G.; Gerenser, L. J.; Gardner, S. A. *J. Am. Chem. Soc.* **1979**, *101*, 6880.

(42) Andersson, S. L. T.; Watters, K. L.; Howe, R. R. *J. Catal.* **1981**, *69*, 212.

(43) Wagner, C. D.; Zatko, D. A.; Raymond, R. H. *Anal. Chem.* **1980**, *52*, 1445.

Table IV. XPS Data of CoO, Co_3O_4, and O_2-Treated Catalyst

sample	$2p_{3/2}$	sat. position, eV	ΔE_{s-o}, eV	ref
CoO	782.5[a]	4.7, 9.2	15.0	19b
	780.3[a]	5.5	15.7	19c
	781.1[a]	6.2	15.1	46a
	780.5[b]	5.9	15.8	46b
	av 781.1 ± 1.0			
Co_3O_4	779.6[a]	9.5	15.0	19c
	780.3[a]		15.1	46a
	779.6[b]	9.9	14.9	46b
	av 779.8 ± 0.4			
O_2-treated catalyst	780.8[c]	6.2	15.2	this work

[a] Referenced to C 1s at 285.0 eV. [b] Referenced to Co $2p_{3/2}$ (metal) at 778.2 eV. [c] Referenced to Al 2s at 119.0 eV.

gun energy and emission were kept the same for all samples; (2) we have already noted the heterogeneous mirroring on the surface of this sample, presumably giving rise to conducting regions; (3) the low-energy peak in the O 1s and LIMS data suggests the presence of charge-carrying alkali cations. Wagner et al.[44] have noted the effects of charging of a thin Al_2O_3 film on Al metal. Thus, the Al 2s binding energy of insulated Al_2O_3 regions decreases from 123.6 to 115.6 to 113.6 eV as one proceeds from no neutralization to moderate neutralization to excessive neutralization while the Al 2s binding energies of Al_2O_3 (in electrical contact with the Al substrate) and the Al substrate remain fixed at 120.1 and 117.9 eV, respectively. The shoulder at 119.0 eV is due to Al_2O_3, for which charge compensation is appropriate, while the more intense band at 116.7 eV is due to Al^{3+} in Al_2O_3, which is in contact with conducting regions on the surface and so excessive charge compensation occurs. Reduction of Al^{3+} to Al metal is unlikely to account for the 116.7-eV band because of the large reduction potential, $E^\circ = -1.71$ V. Further, the Al 2s binding energy for a clean Al is 117.7 eV.[45] This overcharging of the surface also accounts for the large spread of binding energies, 3.4 eV, observed for the O 1s reion and, in particular, the low-binding-energy band at 528.7 eV.

Moderate oxidation (O_2, 30 psi, 250 °C) of the catalyst after one F-T cycle results in an olive green material. The XPS of the Co 2p region (Figure 3d) indicates that the metallic cobalt species are readily oxidized by this treatment. The spin–orbit splitting, 15.2 eV, would suggest that the extent of oxidation is to Co(III); however, the presence of moderately intense satellite structure suggests that this consideration alone is not definitive in assigning the oxidation state of cobalt on this oxidized sample. Comparison of the $2p_{3/2}$ binding energy, satellite line separation, and spin–orbit splitting of the common cobalt oxides, CoO and Co_3O_4, with those of our oxygen-treated catalyst is shown in Table IV. A brief inspection of Table IV indicates that there is great variation in the measured spin–orbit splitting of CoO as values range from 15.0 to 15.8 eV. On the average, the $2p_{3/2}$ binding energy of CoO is 1.3 eV higher than that of Co_3O_4, and CoO shows smaller satellite line separations. Data for our postreaction oxidation treatment is in close agreement with that of Oku et al.[46a] for CoO. Although we do not completely rule out the presence of some Co(III), the color of the catalyst after oxidation is that of CoO. Because CoO has Co(II) ions in octahedral sites, a change in coordination about the Co(II) has occurred upon oxidation.

Acknowledgment. The authors wish to extend special thanks to Dr. David Hercules and his graduate student, C. P. Li, of the University of Pittsburgh for providing the LIMS data. We also thank Randy Scott at the Electron Microscopy Center, Texas A&M University, for providing the TEM data. We gratefully acknowledge the Center of Energy and Mineral Resources (CEMR) at Texas A&M University for their financial support.

Note Added in Proof. While this paper was in press, Ferkul et al. reported on the heterogeneous F-T reaction using supported $Co_4(CO)_{12}$ in a flow reactor system. These workers also observed typical F-T product distributions when γ-Al_2O_3 was used as a support.[47]

Registry No. Dodecacarbonyltetracobalt, 17786-31-1; cobalt, 7440-48-4; carbon monoxide, 630-08-0.

(44) Wagner, C. D.; Riggs, W. M.; Davis, L. E.; Moulder, J. F. "Handbook of X-ray Photoelectron Spectroscopy"; Muilenberg, G. E., Ed.; Perkin-Elmer Corporation: Eden Prairie, MN, 1979; p 26.
(45) Barrie, A. *Chem. Phys. Lett.* **1973**, *19*, 109.
(46) (a) Oku, M.; Hirokawa, K. *J. Electron Spectrosc. Relat. Phenom.* **1976**, *8*, 475. (b) Chaung, T. J.; Brundle, C. R.; Rice, D. W. *Surf. Sci.* **1970**, *43*, 625.
(47) Ferkul, H. E.; Berlie, J. M.; Stanton, D. J.; McCowan, J. D.; Baird, M. C. *Can. J. Chem.* **1983**, *61*, 1306.